Multinuclear solid state NMR studies of the Guest-Mediated Zeolite Crystallization
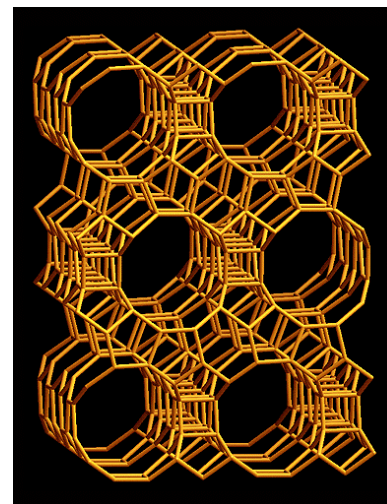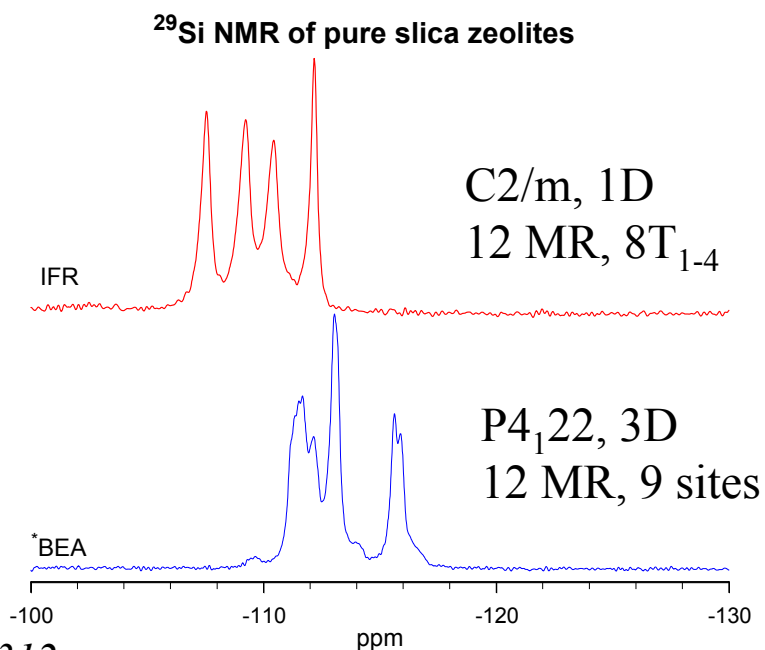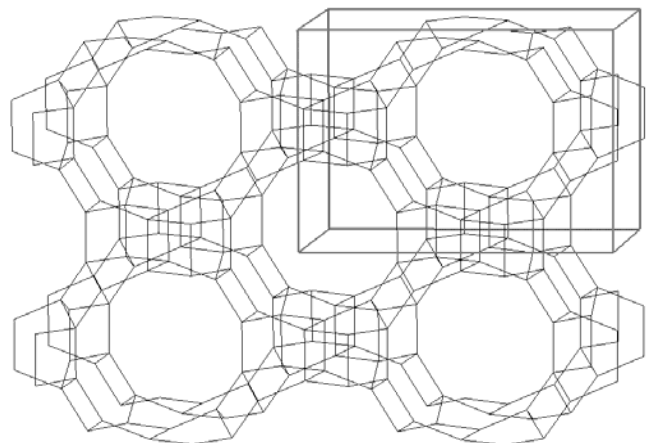
Son-Jong Hwang[1] and S.I. Zones[2]

[1]Division of Chemistry and Chemical Engineering, California Institute of Technology, Pasadena, CA 91125, USA.

[2]Chevron Research and Technology Company, P.O. Box 1627, Richmond, CA 94802, USA.

I. Introduction

The present work focuses on the understanding of the mechanistic difference in the process of zeolite crystallization for a system that the substituting trivalent metal ions determine the product selectivity. The synthetic route employs boron or aluminum metal ions and results in the formation of two different zeolite structures, SSZ-42 (IFR) and beta (BEA) zeolite, respectively, when all the other components remain the same. IFR structure type has 1D pore system with 12 MR while BEA structure has intersecting 12 MR in 3D. Understanding of the mechanistic difference for boron vs aluminum should provide us with better prediction of product selection in the discovery of new zeolites. Multinuclear NMR methods were employed to follow the structural changes around the organo-cation guest molecule (N-Benzyl DABCO) as a function of crystallization time as well as the changes after calcination. The powder recovered at each point of reaction time frame was also analyzed with XRD, NMR, and elemental analysis.

^{29}Si NMR of pure slica zeolites

IFR

C2/m, 1D
12 MR, $8T_{1-4}$

P4$_1$22, 3D
12 MR, 9 sites

*BEA

-100   -110   -120   -130
ppm

[1]Zones, et al. *Chem. Eur. J. 1998, 4, 1312*

II. Experimental

Sample Preparations

Figure 1. Structure of the SDA (N-Benzyl-DABCO) used in this work.

Table 1. Reagents and synthesis conditions used in the comparative runs of SSZ-42 and beta (150° C, 43 rpm)

Ratio	SSZ-42 RUN	BETA RUN
N-Benzyl-DABCO/SiO_2	0.20	0.20
NaOH/SiO_2	0.10	0.10
SiO_2/Al_2O_3 (SAR)	0.00	35*
SiO_2/B_2O_3	35*	0.00
NET OH⁻ /SiO_2	0.30	0.30
H_2O / SiO_2	44*	44

* Except when values have been varied in separate series

Table 2. Elemental analyses for recovered run products (B series)

Sample #	RUN TIME	XRD
B1	0 days	Amorphous
B2	1 day	Amorphous
B3	2 days	20% SSZ-42
B4	3 days	SSZ-42
B5	6 days	SSZ-42

Table 3. Elemental analyses for recovered run products (Al series)

Sample #	RUN TIME	XRD
A1	0 days	Amorphous
A2	1 days	Amorphous
A3	7 days	Amorphous
A4	9 days	beta

NMR   Solid state NMR spectra were obtained using Bruker DSX 200 (B_o=4.7 T) and DSX 500 (B_o=11.7 T) spectrometers and a 4mm CPMAS probe. Detail NMR operating parameters are given in the result section.

III. Results and discussion

Crystallization : As were compiled in Table 1, for the two synthesis systems the borosilicate (BSSZ-42) reaction crystallizes much more rapidly to form SSZ-42 while aluminosilicate(Al-Beta) starts crystallizing Beta after 7 days.
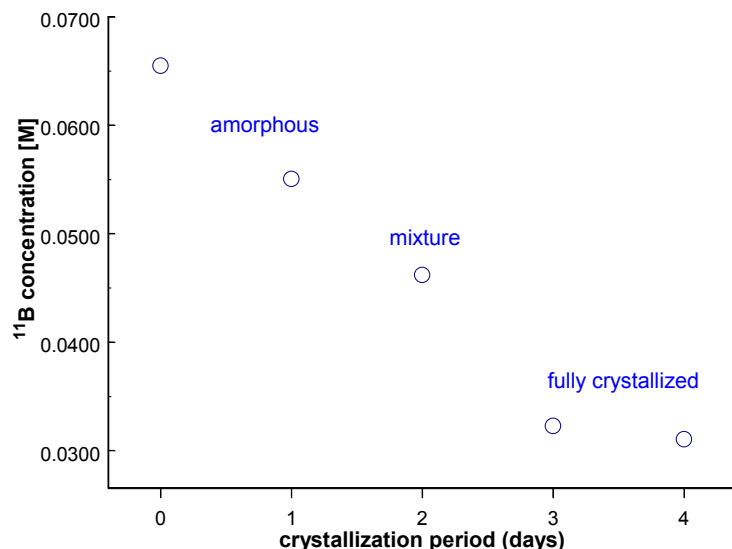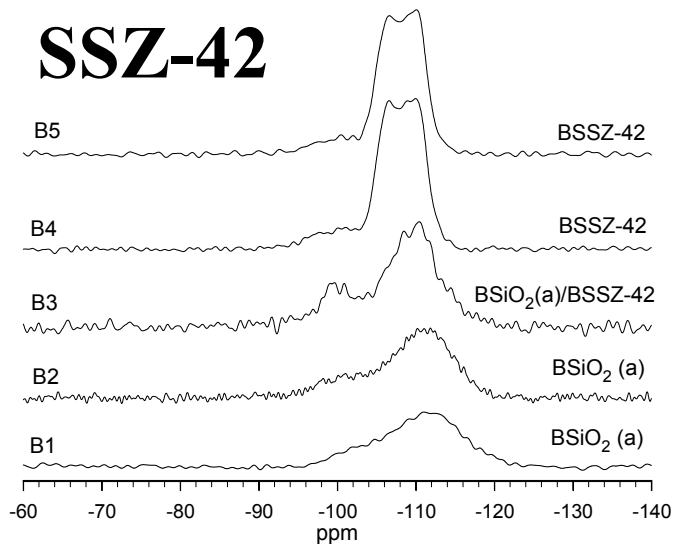
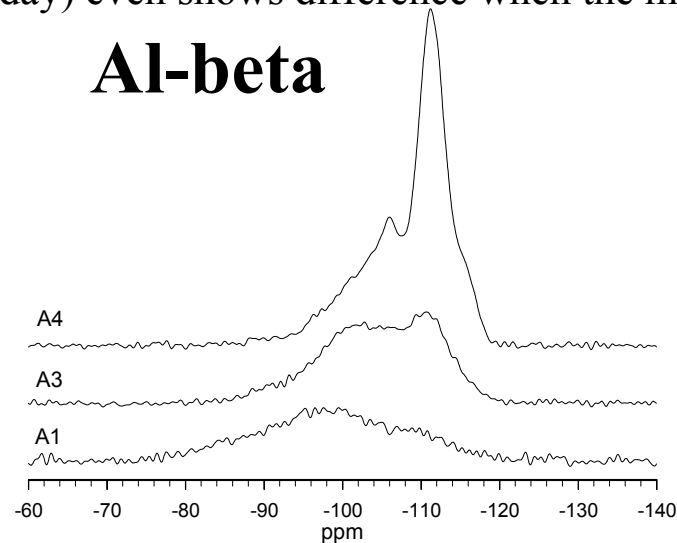Fig. 2 shows the change of [11]B concentration of the supernatant during the crystallization period.

Crystallization takes place with incorporation of boron in the framework. ^{11}B MAS NMR spectra also measure the maturity of the crystallization process. About half of the boron remains unreacted.

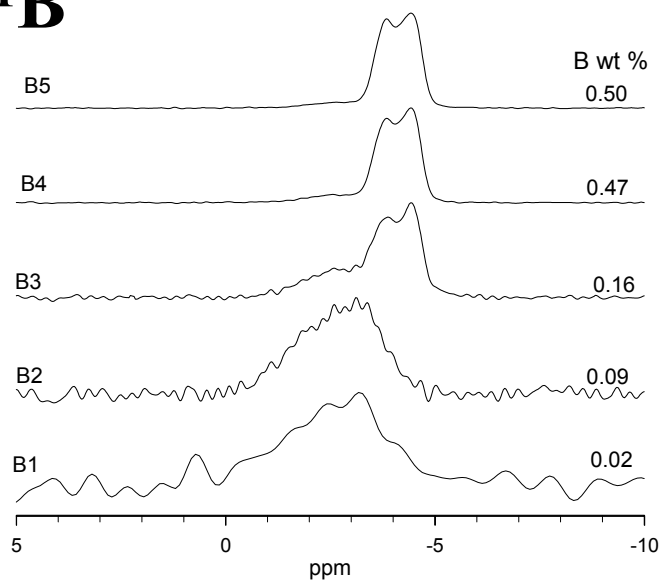**Figure 2**. [11]B concentration in supernatant

NMR of as prepared powders: ^{29}Si NMR and NMR on trivalent metals of powder materials recovered at each time point eminently reveal the conversion to crystalline phases from amorphous phases. Note that ^{29}Si NMR of powders before any thermal treatment (0 day) even shows difference when the metals
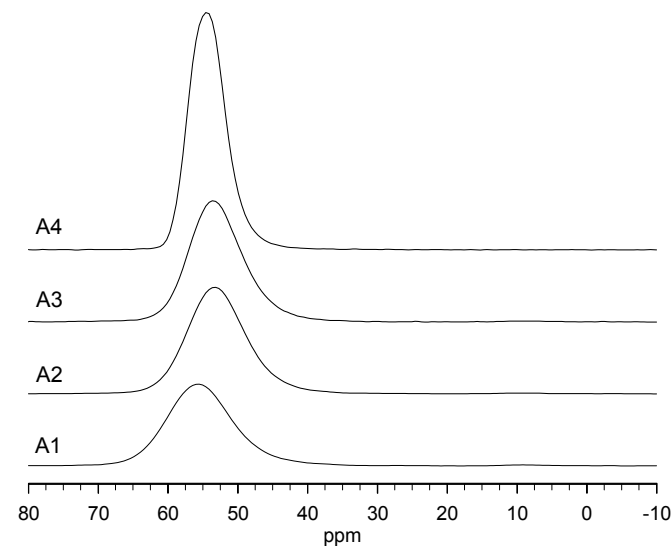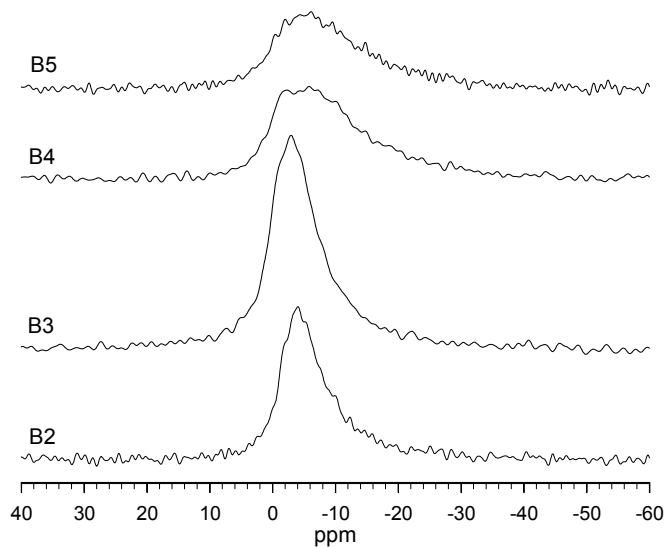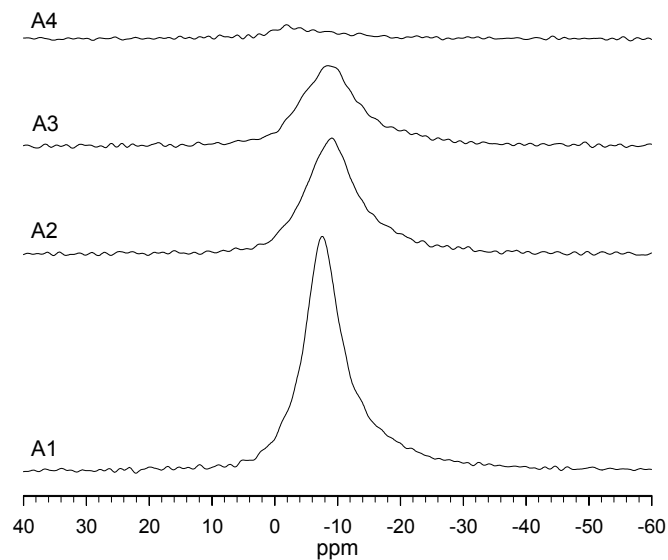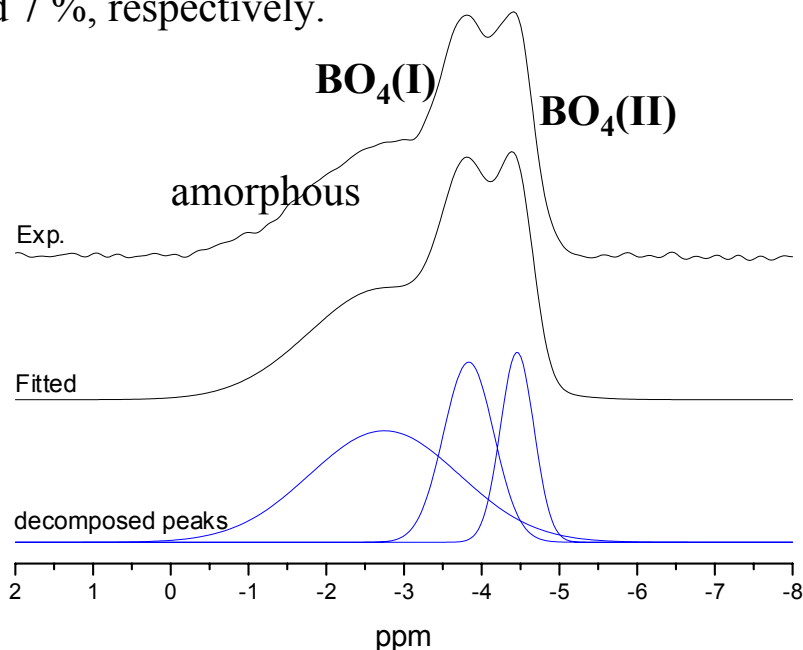
^{23}Na

are different. The beta structure starts with much more of Q^3 site (~-100 ppm) compared to SSZ-42 structure. Second, the kinetics of metal incorporation is different. Boron gets inserted into the framework progressively as was indicated in Figure 2. The content of aluminum, however, is rather constant regardless of the thermal treatment or the extent of crystallinity (crystallization time). Both ^{1}H and ^{13}C NMR indicate that the amount of SDA found in the recovered powders for both structures increases as a function of the reaction time. ^{23}Na NMR measurements reveal in and out of Na ions as the nucleation proceeds. The role of Na^+ ion is the counter ion for the negatively charged metal ions when the positively charged SDA is not available. The dramatic decrease of Na content for beta structure at the end indicates that the SDA moves progressively to Al locations and replace Na ions.

Boron Doublet

Unlike broad feature of Al signal, ^{11}B NMR spectra of SSZ-42 powders consist of at least three components, and decomposition using a peak fitting program reveals the distribution of boron atoms among the sites in the framework.

•Boron atoms are found to be all tetrahedrally coordinated (BO_4^-, -3 ~ -5 ppm) and in two different environments with their chemical shift change is only 0.6 ppm. Note that four different T sites are present in the structure (see ^{29}Si NMR).

•Borons in amorphous phase render a featureless broad line (FWHM~300 Hz at 11.7 T). Quantitation by spectral line fittings yields that the portions of amorphous phase for sample B3 and B5 are 46 % and 7 %, respectively.

•The relative intensity ratios $BO_4(I)/BO_4(II)$ approaches to 1 as the crystallization completes. are 1.3 and 0.9 for sample B3 and B5, respectively.

Figure 3. Experimental and simulated ^{11}B MAS NMR spectra of B3 compound obtained using Bruker DSX500 (ν_r =12 kHz).

•It is unrealistic to predict that only two of the four T sites are selectively replaced by boron atoms. In order to better characterize the boron doublets, several boron containing zeolites were synthesized and the similar boron NMR measurements were made (see Fig 4). SSZ-33 (CON) has seven T sites. It is clear that the boron doublet is unique to IFR structure.

•SSZ-42 was calcined, and also boron atoms were extracted with acetic acid treatment (Fig. 5). $BO_4(II)$ gets preferably removed upon calcination. The acetic acid treatment at 135 C removes most of $BO_4(I)$ sites, but both sites still exist. When the compound was heated at 185 C in acetic acid media, $BO_4(II)$ was completely removed.
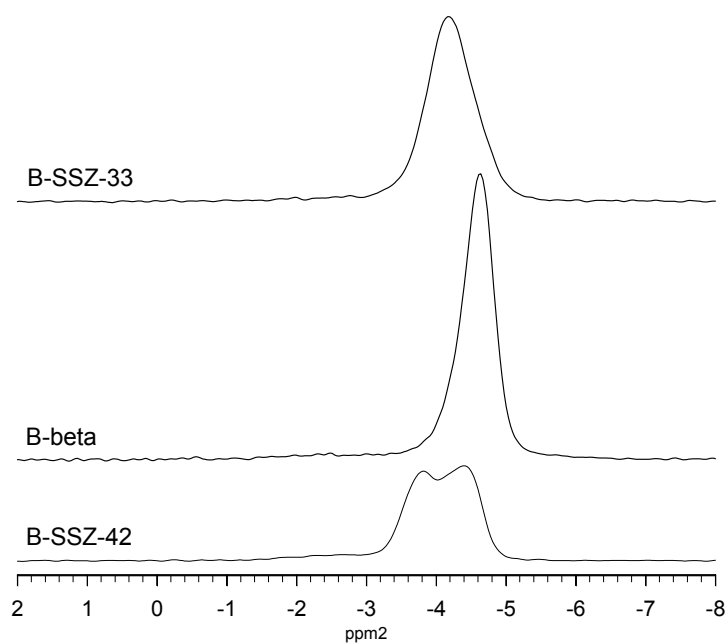

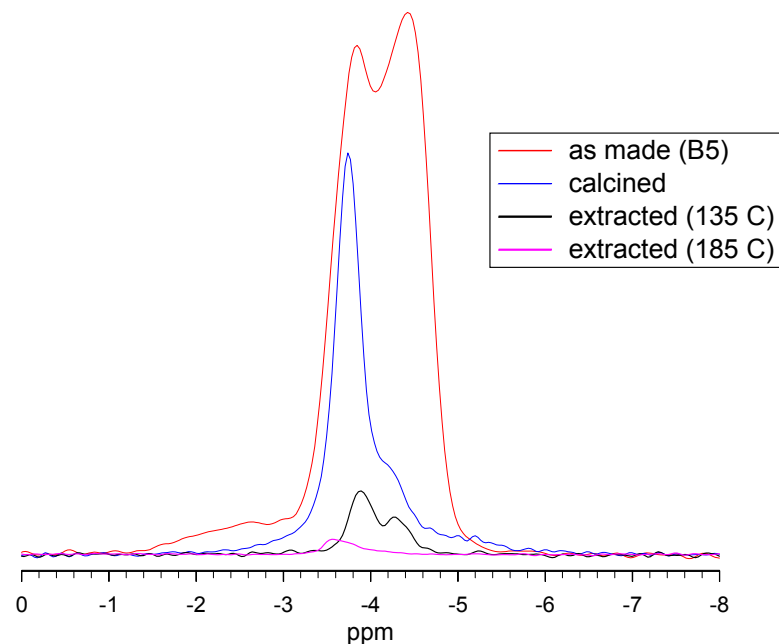**Figure 4**. ^{11}B NMR of different zeolite Structures.

Figure 5. ^{11}B NMR of B-SSZ-42 after several treatments.

•The negatively charged boron sites can be compensated by either the SDA or Na$^+$, and the counter ions can induce the chemical shift difference of boron atoms. In order to investigate this, another synthetic route employed NH$_4^+$ as the counter cation, and SDA$^+$ was more introduced to the system. The resulting ^{11}B NMR spectra and the decomposition are seen in Fig. 6. The boron doublets are still present regardless of the changes in the counter ions although the relative intensity ratio and the line width are slightly varied. An extra resonance was needed in the fitting for the case of more SDA used.
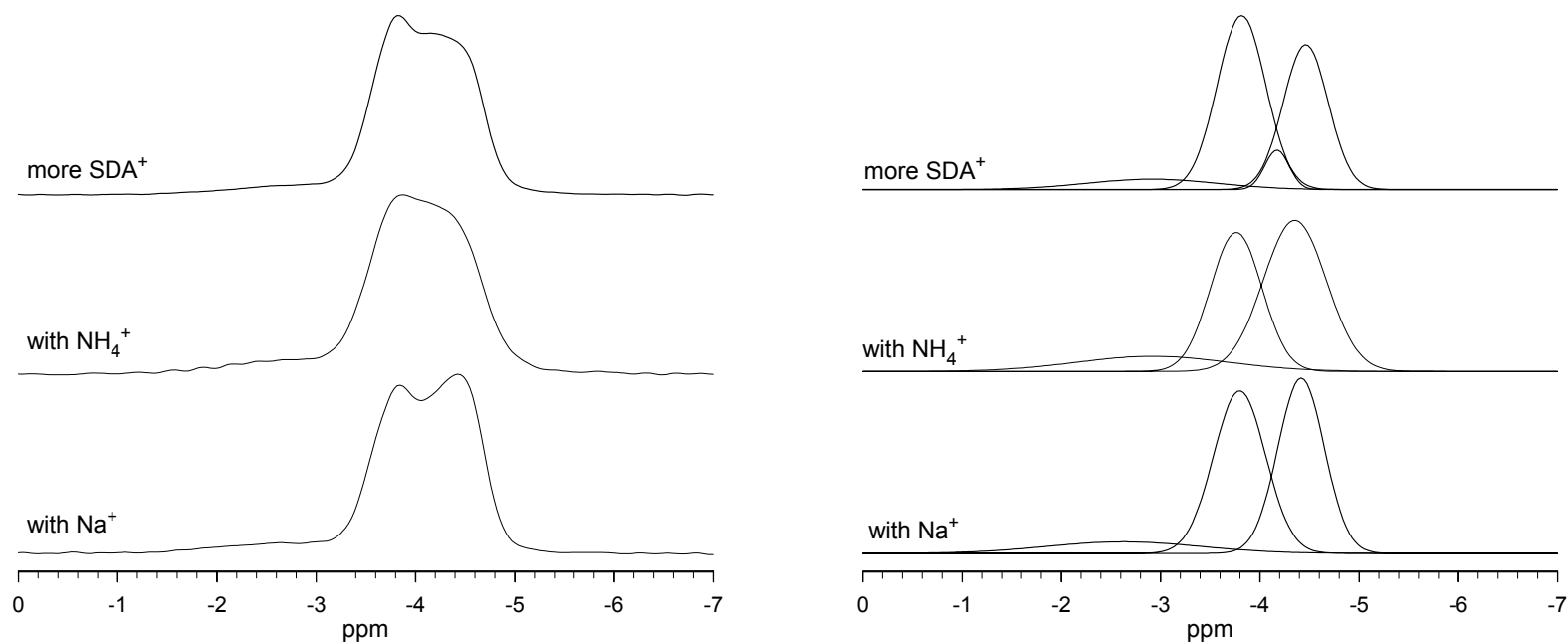

Figure 6. ^{11}B NMR of B-SSZ-42 prepared with different positive counter ions and decomposition of lines.

^{11}B CPMAS and 2D WISE

Further characterization was made for the boron doublet. Figure 7 shows ^{11}B CPMAS NMR results as a function of contact time and a 2D WISE spectrum of as made B3 (BSSZ-42). Proximity from the SDA can be obtained qualitatively: Possible different BO_4(I) and BO_4(II) locations in the framework.

• The CP dynamics distinguishes the proton source.

BO_4(amorphous) T_{BH}=140 us, $T_{1\rho}$=1.87 ms (from sample B2); mostly water or OH groups

BO_4(crystalline) T_{BH}=530 us, $T_{1\rho}$=22.1 ms (measured from sample B5) : SDA

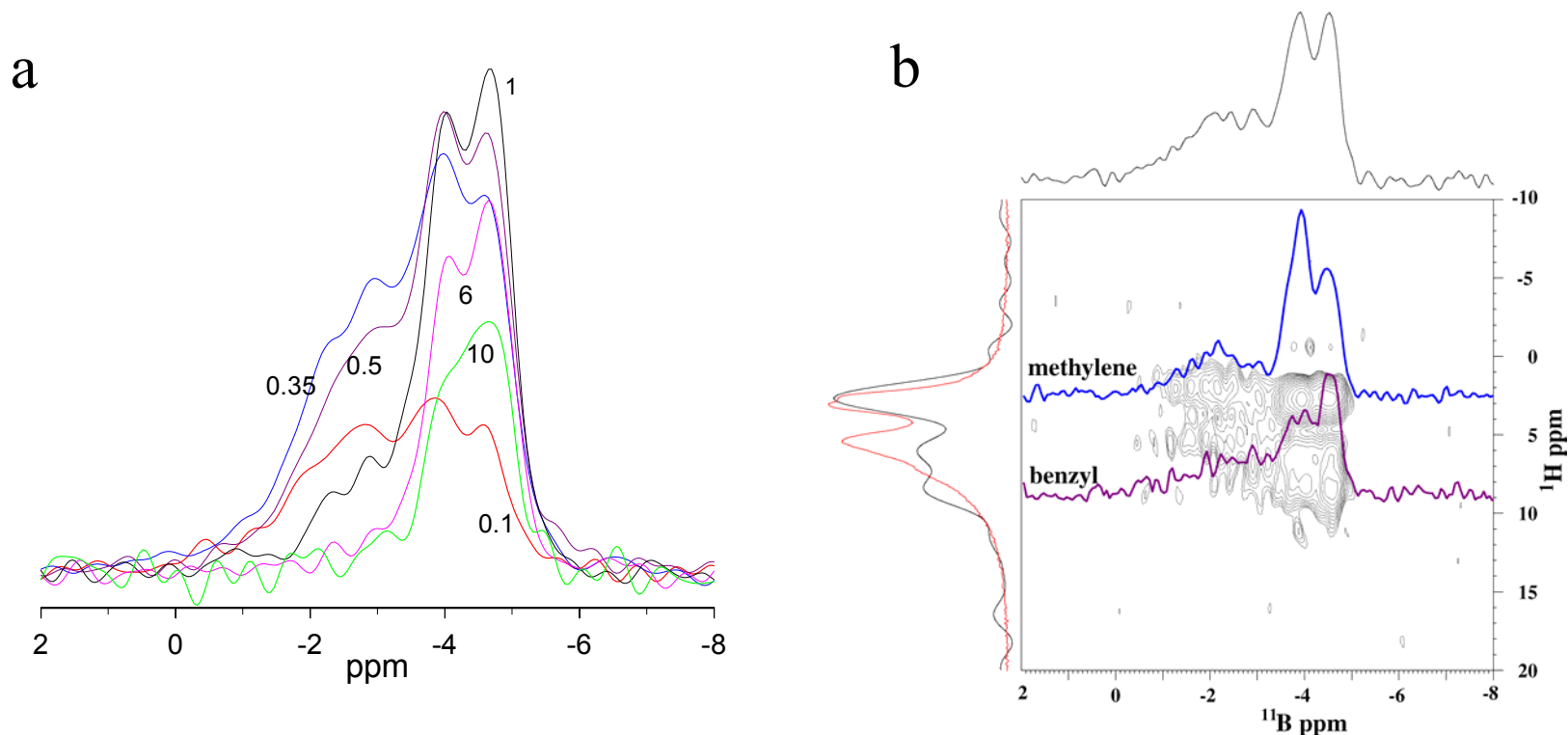**Figure 7.** ^{11}B CPMAS NMR. a. sample B3. CP contact times (in ms) by each line. b. 2D WISE (CP contact time=0.2 ms) on sample B3(BSSZ-42). ^{1}H MAS spectrum (red) as well as slices for aliphatic and aromatic protons are overlapped onto the 2D contour plot for comparison.

•As shown in Figure 7b, 2D WISE spectrum provide the proximity information between the $BO_4(I)$ and $BO_4(II)$. $BO_4(I)$ seems to be located closer to the aliphatic group of SDA while $BO_4(II)$ does so to the aromatic ring of SDA.

•SDA with the perdeuterated benzyl ring was used to synthesize another BSSZ-42, and its ^2H MAS NMR and $^{11}B\{^1H\}$ CPREDOR experiments were performed. ^2H MAS indicates that benzyl ring has very limited motion even at room temperature. The REDOR effect support the conclusion from the WISE experiment that the $BO_4(I)$ site is closer to the aliphatic part of the SDA. Any quantitative analysis of the $^{11}B\{^1H\}$ REDOR experiment is not made.
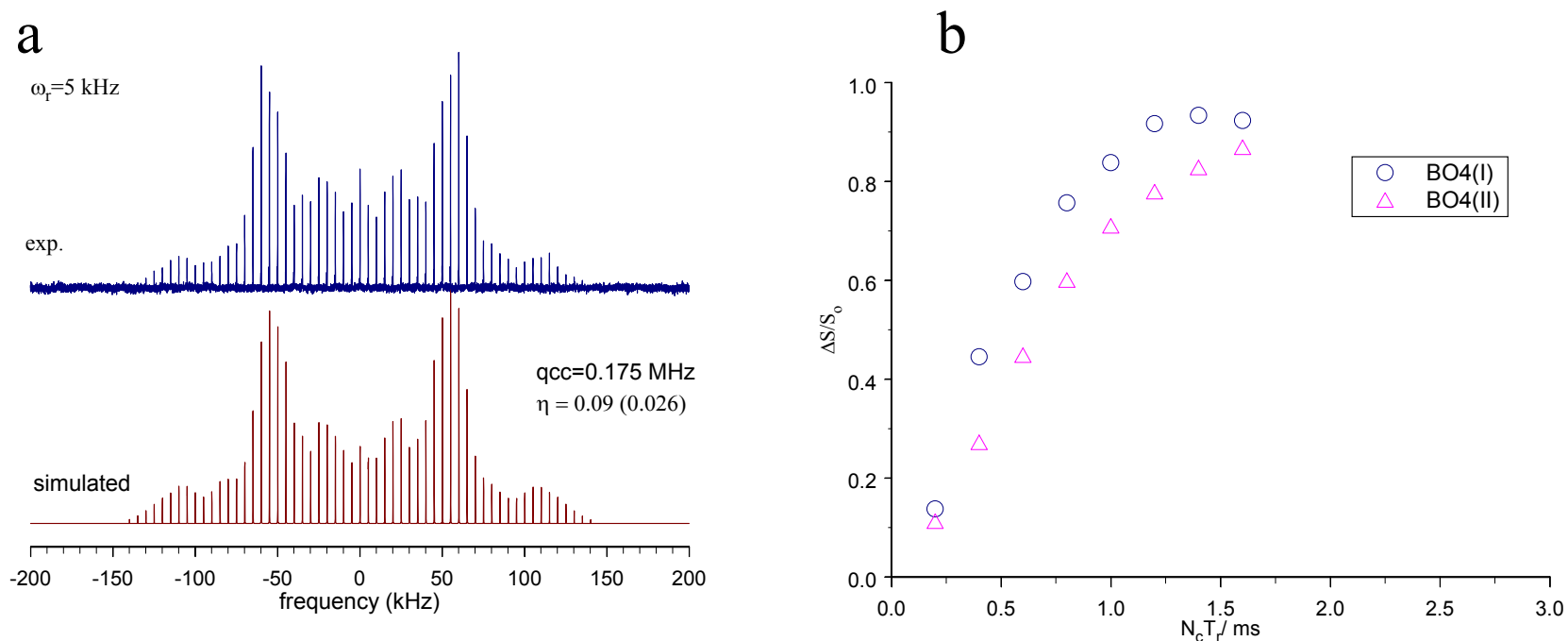

Figure 8. a. ^2H MAS NMR spectrum and simulation (5 kHz spinning at 11.7 T).
b. $^{11}B\{^1H\}$ CP-REDOR experiment (CP contact time=0.5 ms, υ_r=10 kHz, 11.7 T).

b. after calcination ^{11}B MAS NMR spectra of two calcined (4 h at 540° C) zeolites are shown in Figure 9a. No additional dehydration was performed. Formation of trigonally coordinated boron (BO_3) (quadrupolar power pattern at 8-0 ppm, $BO_3(II)$) is seen for both samples after calcination while the conversion in sample B3 is negligible. Another type of trigonal site(20-10 ppm, $BO_3(I)$) is also visible in B5. A few interesting observations are

• The conversion of BO_4 to BO_3 sites upon calcination is markedly higher for the crystalline BSSZ-42 (sample B5) than that found for sample B3 (amorphous mixture).
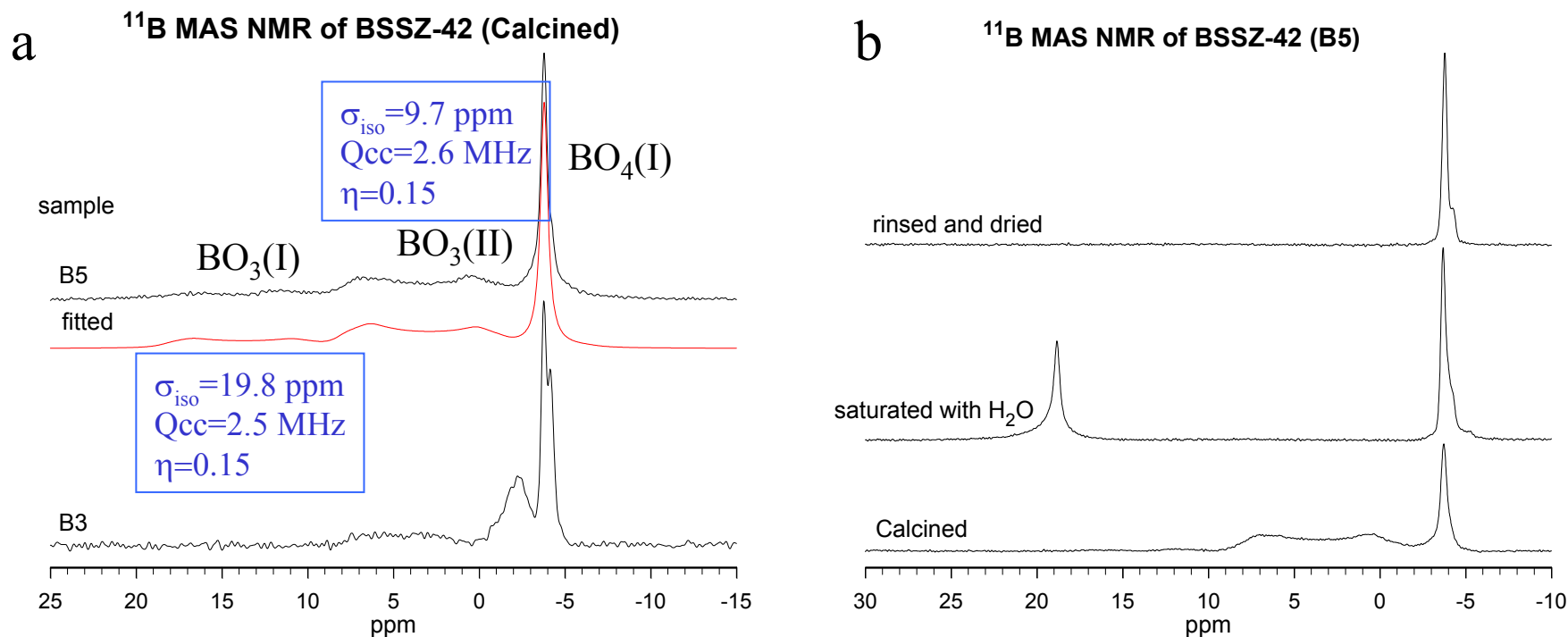

Figure 9 ^{11}B MAS NMR spectra (DSX 500, v_r=12 kHz) a. after calcination. b. effect of hydration

•Integration of the signal estimates the $[BO_3]/[BO_4]$ = ~1.5 for sample B5 (crystalline BSSZ-42). $BO_4(II)$ sites shows a nearly complete conversion to BO_3 unit while $BO_4(I)$ show about 50 % conversion. Correlation can be made based on the quantitation: $BO_4(I)$=> $BO_3(I)$ and $BO_4(II)$=> $BO_3(II)$

•In sample B3, all the lines get narrowed significantly by calcination. The severe change in overall spectral lineshape is simply associated with the different extent of line narrowing among the sites. The relative intensity ratios are found to remain unchanged. No selective destruction of $BO_4(II)$ was observed.

•In the previous report by Fild et. al.[2], trigonal site $BO_3(II)$ was assigned to be a trigonal site in the frame work while the other one ($BO_3(I)$ was to be outside of the framework. Note that the quantity of $BO_3(I)$ is negligible. The presence of both BO_4 and BO_3 units are also consistent with the previous result[1] because both Na^+ and H^+ might act as the counterions.

•Interestingly hydration of calcined sample (see Figure 9-b) resulted in the formation of a peak at 18.5 ppm (B_2O_3 in aqueous phase) as well as some recovery of the tetrahedral sites (~20 % of $BO_3(II)$ site) as indicated by peak growth both at -3.8 and -4.5 ppm. 80 % of the trigonal sites are converted to form 18.5 ppm peak, which is not consistent with the postulation[1] (see above) if $BO_3(II)$ is bridged by -Si-O-B bond in the framework. Peak at 18.5 ppm was negligibly small for hydration of sample B3 (amorphous mixture) as can be expected from the small quantity of BO_3 sites (spectra not shown).

•Rinsing and drying of hydrated B5 (see Figure 9-b) lead to observation of the top spectrum in Figure 9-b, clearly indicating that the 18.5 ppm peak can be washed out. This result implies that significant portion of the trigonal sites created by calcination are already outside the framework or weakly bridged to the framework and therefore can be removed by hydration.

[2]Chirstian Fild, et al. Phys. Chem. Chem. 2000, 2, 3091
[3]Christian Fild, et al. Angew. Chem. Int. Ed. 1998, 37, 2505.
[4]Christian Fild, et al. J. Am. Chem. Soc. 122, 12590 (2000).

IV. Summary

1. Understanding of mechanistic difference in synthetic of BSSZ-42 and Al-Beta was attempted by studying recovered powders using solid state NMR methods.

2. ^{11}B NMR methods were very sensitive to identify the coordination geometry of boron atoms in/outside the framework of forming zeolite during the crystallization process. Lattice substitution of boron atoms resulted in the formation of two distinctive BO_4 (tetraherdally coordinated borons: Boron Doublets) sites in the SSZ-42 framework.Such doublets were found to be so far unique to the IFR structure. One of the site shows a strong selectivity toward to forming BO_3 units upon calcination, then can be easily removed by hydration and rinsing. Such a discrepancy was not observed for the amorphous mixture of the same structure. Identification of the doublets is under progress.

3. Similar dealumination reaction occurred and two tetrahedral Al sites were observed when Al-Beta was calcined (results not shown).

Future work includes getting information about spatial proximity from the incorporated metal ions to the SDA as well as other changes during the aging process which can help us to understand the pathway better.

V. Acknowledgements